DALTON
FULL PAPER

Syntheses and crystal structures of the molecular conductors $Z[Pd(dmit)_2]_2$ {$Z = (Me_3NEt)^+$, $(MeNEt_3)^+$, $(NEt_4)^+$} and their precursors $Z_2[Pd(dmit)_2]$

Fang Qi,*[a,b] Thomas C. W. Mak,[b] Zhou Zhong-Yuan,[b] Yang Qing-Chuan,[b] Liu Zhi,[a] Yu Wen-Tao,[a] Zhu Dao-Ben[c] and Jiang Min-Hua[a]

[a] *State Key Laboratory of Crystal Materials, Shandong University, Jinan, Shandong, 250100, P. R. China.. E-mail: fangqi@icm.sdu.edu.cn*
[b] *Department of Chemistry, The Chinese University of Hong Kong, Hong Kong, P. R. China*
[c] *Institute of Chemistry, The Chinese Academy of Science, Beijing, 100080, P. R. China*

Received 3rd July 2001, Accepted 4th February 2002
First published as an Advance Article on the web 7th March 2002

Electrically conductive platelet crystals of $Z[Pd(dmit)_2]_2$ [$Z = (Me_3NEt)^+$, $(MeNEt_3)^+$, $(NEt_4)^+$], as well as their precursors $Z_2[Pd(dmit)_2]$, have been synthesized by a non-electrochemical method and their structures have been determined. The single-crystal conductivities at a direction on the cleavage surface at room temperature were measured to be 58 Ω^{-1} cm^{-1} for $(Me_3NEt)[Pd(dmit)_2]_2$, 5.0 Ω^{-1} cm^{-1} for $(MeNEt_3)[Pd(dmit)_2]_2$ and 2.2 Ω^{-1} cm^{-1} for $(NEt_4)[Pd(dmit)_2]_2$, respectively. This sequence of conductivity is agreement with the sequence of structural two-dimensionality of these three complexes. The resistivity–temperature curves reveal the semiconducting behavior of the above complexes, which show very narrow band gaps. The structure analysis results reveals that when the size of cation Z in $Z[Pd(dmit)_2]_2$ is finely tuned [$(Me_4N)^+ \longrightarrow (Me_3NEt)^+ \longrightarrow (Me_2NEt_2)^+ \longrightarrow (MeNEt_3)^+ \longrightarrow (NEt_4)^+$], the corresponding complexes belong to the same structural motif and each individual possesses some special structural characteristics. Subtle structural difference in this group of complexes can severely influence their measured conductivities and significantly influence their calculated band structures.

1 Introduction

Up to now, $Z[M(dmit)_2]_2$-type complexes (dmit = $C_3S_5^{2-}$ = 4,5-dimercapto-1,3-dithiole-2-thione; Z = monovalent cation) continue to be the most dominant family in the various kinds of molecular-based electrically conductive coordination compounds. A total of seven examples of this kind of complex have been reported to be superconductors.[1–6]

Chemical modifications aimed at exploring new superconductors of the kind have been limited to: (1) modification of the dmit ligand, (2) exchange of the metal ion M for another and (3) substitution of the closed-shell or open-shell cation Z one for another. The strategy of replacing sulfur in dmit ($C_3S_5^{2-}$) with more polarizable selenium, such as the syntheses of the $C_3S_3Se_2^{2-}$ (dsit) ligand and the conductive complex $(Me_4N)[Pd(dsit)_2]_2$,[7] is significant, but dsit and all the other selenium-containing analogues have not been proved to be superior to dmit. The dmit ligand can coordinate with variety of metal ions, but only the complexes of Ni, Pd, Pt and Cu proved to be promising, and only the complexes of Ni, Pd have demonstrated superconductivity.[1–6] The practice of changing the cation Z is simple, but the results are not trivial, since small structural perturbations may result in greatly enhanced conductivity. For example, $(NEt_4)[Ni(dmit)_2]_2$[8] is a semiconductor and $(Me_2NEt_2)[Ni(dmit)_2]_2$[9] shows metallic behavior, similarly, $(Me_4N)[Ni(dmit)_2]_2$[2] is a superconductor at 5 K under 7 kbar whereas α-(EDT-TTF)$[Ni(dmit)_2]_2$,[3] with open-shell organic cation EDT-TTF, shows superconductivity under ambient pressure.

Although the cation itself is not the main conducting component in the crystal, it does play a vital role in controlling the packing details of the conducting component, $[M(dmit)_2]^{0.5-}$, and therefore in engineering the energy band structure of the crystal. In this paper, the syntheses, structures and electrical conducting properties of the title complexes are reported. Among them, $(NEt_4)[Pd(dmit)_2]_2$ was first synthesized in 1987 by Groenveld and coworkers by different method from the ours,[10] and was reported to have the same structure but to show different temperature dependence of the conductivity compared to our results (see section 3.2). Tetraalkylammonium cations with tiny differences in size have been chosen to combine with the same anion, $[Pd(dmit)_2]^{0.5-}$, in order to finely tune the structures and to make some structure–property conclusions. Instead of the commonly used electrochemical oxidation method, a reproducible chemical oxidation method has been developed.

2 Experimental

2.1 Syntheses of the precursors $(Me_3NEt)_2[Pd(dmit)_2]$, $(MeNEt_3)_2[Pd(dmit)_2]$ and $(NEt_4)_2[Pd(dmit)_2]$

To a dry two-neck flask containing 2.0 mmol (813.2 mg) of orange bar-shaped $dmit(COPh)_2$ [4,5-bis(benzylthio)-1,3-dithiole-2-thione] crystals, which were synthesized by the literature method,[11] 16 mL of 1 M NaOEt in EtOH was added under nitrogen at room temperature with stirring. Immediately, the rose-colored dmit, which is unstable in air, was released and the mixture was stirred for 20 min to ensure all the $dmit(COPh)_2$ dissolved and reacted. Then, a 50 mL EtOH solution containing 1.2 mmol (212.8 mg) $PdCl_2$ and 2.0 mmol (899.3 mg) NaI (to enhance the solubility of the $PdCl_2$) was added. In the course of dropping of a 20 mL EtOH solution containing 3.0 mmol (645.3 mg) $(Me_3NEt)I$, purple microcrystals of $(Me_3NEt)_2[Pd(dmit)_2]$ precipitated out. Large rose-colored platelet crystals, suitable for X-ray structure determination, were obtained by recrystallization in a mixture of acetone and ethanol in a vacuum desiccator over $LiAlH_4$ over the course of

DOI: 10.1039/b105854c

2 days. Yield: 53%. Mp: 243–245 °C. Found: C, 28.26; H, 3.67; N, 3.24; S, 47.22%. $C_{16}H_{28}N_2PdS_{10}$ requires C, 28.45; H, 4.18; N, 4.15; S, 47.47%. IR (KBr; cm^{-1}): ν(C=C) 1442; ν(C=S) 1048w, 1025m, 1012s.

Similarly, $(MeNEt_3)_2[Pd(dmit)_2]$ crystals were synthesized when $(MeNEt_3)I$ was used as the precipitant. Yield: 57%. Mp: 239–241 °C. Found: C, 32.80; H, 4.68; N, 4.21; S, 43.04%. $C_{20}H_{36}N_2PdS_{10}$ requires C, 32.83; H, 4.96; N, 3.83; S, 43.83%. IR (KBr; cm^{-1}): ν(C=C) 1444s; ν(C=S) 1047s, 1016s.

When $(NEt_4)Br$ was used, parallelepiped crystals of $(Et_4N)_2[Pd(dmit)_2]$ were obtained. Yield: 51%. Mp: 230–232 °C. Found: C, 34.77; H, 4.37; N, 4.09; S, 41.39%. $C_{22}H_{40}N_2PdS_{10}$ requires C, 34.78; H, 5.31; N, 3.69; S, 42.21%. IR (KBr; cm^{-1}): ν(C=C) 1439s; ν(C=S) 1046s, 1026s.

2.2 Syntheses of $(Me_3NEt)[Pd(dmit)_2]_2$, $(MeNEt_3)[Pd(dmit)_2]_2$ and $(NEt_4)[Pd(dmit)_2]_2$

Half-charged anionic $[M(dmit)_2]^{0.5-}$ was generated by removing the negative charge from dianionic $[M(dmit)_2]^{2-}$ using appropriate electron acceptors. A diffusion reaction technique has been developed by using a kind of three-compartment cell. Each of the compartments, which have volumes of about 20 mL, were partially isolated by glass frits. All of the diffusion reaction processes were kept free from oxygen and moisture. The solvent was CH_3CN which had been freshly distilled over CaH_2 and under N_2 before use. The yields of the following target compounds are nearly 100%. All the samples for IR spectroscopy were made from individual single crystals, so phase impurity, which may exist in an amount of product, can be precluded.

2.2.1 $(Me_3NEt)[Pd(dmit)_2]_2$. 0.2 mmol (25.6 mg) of colorless tetracyanoethylene (TCNE), which had just been sublimed, was put in the left part of the three-compartment cell and 0.05 mmol (32.3 mg) of platelet crystals of $(Me_3NEt)_2[Pd(dmit)_2]$ in the right. Under an N_2 atmosphere, the three compartments were filled with freshly distilled CH_3CN. The cell was then sealed and left in the dark. After 9 days diffusion and reaction, shiny black platelet crystals, which were identified as $(Me_3NEt)[Pd(dmit)_2]_2$ by X-ray structural analysis, were obtained. Found: C, 18.45; H, 1.51; N, 1.21; S, 58.67%. $C_{17}H_{14}NPd_2S_{20}$ requires C, 18.79; H, 1.30; N, 1.30; S, 59.03%. IR (KBr; cm^{-1}): ν(C=C) 1327w, 1289s; ν(C=S) 1060s, 1043m, 1024w.

2.2.2 $(MeNEt_3)[Pd(dmit)_2]_2$. *Method 1.* 0.1 mmol (27.3 mg) of purple-colored ferrocenium tetrafluoroborate $[Fe(C_5H_5)_2]BF_4$, which was synthesized according to the literature method,[12] was put in the left part of the cell and 0.05 mmol (37.9 mg) of platelet crystals of $(MeNEt_3)_2[Pd(dmit)_2]$ in the right. Following the same procedure as above, after 44 days, shiny black platelet crystals of $(MeNEt_3)[Pd(dmit)_2]_2$ were harvested. Found: C, 20.26; H, 1.55; N, 1.23; S, 57.78%. $C_{19}H_{18}NPd_2S_{20}$ requires C, 20.47; H, 1.63; N, 1.26; S, 57.54%. IR (KBr; cm^{-1}): ν(C=C) 1325.5w, 1286.2s; ν(C=S) 1056.9s, 1023.3m.

Method 2. 0.05 mmol (12.7 mg) of I_2, 0.10 mmol (15.0 mg) of NaI and 0.05 mmol (37.9 mg) of $(MeNEt_3)_2[Pd(dmit)_2]$ were put into the left, middle and right sections of the three-compartment cell, respectively. Following the same procedure as above with a reaction time of 22 days, shiny black platelet crystals of $(MeNEt_3)[Pd(dmit)_2]_2$ were obtained. IR (KBr; cm^{-1}): ν(C=C) 1326.0w, 1286.2s; ν(C=S) 1056.2s, 1023.5m. The identity of the products prepared *via* the two methods was supported by their IR spectra.

2.2.3 $(NEt_4)[Pd(dmit)_2]_2$. Using similar methods to those above with the acceptors $[Fe(C_5H_5)_2]BF_4$ (over the course of 45 days diffusion and reaction) or I_2–NaI (over the course of 14 days), shiny black platelet crystals of $(Et_4N)[Pd(dmit)_2]_2$ were obtained. This product can also be satisfactorily synthesized by using tetracyanoquinodimethane (TCNQ) (over 32 days) as the acceptor. Found: C, 20.89; H, 1.65; N, 1.46; S, 56.24%. $C_{20}H_{20}NPd_2S_{20}$ requires C, 21.29; H, 1.79; N, 1.24; S, 56.83%. The IR (KBr) spectra of $(Et_4N)[Pd(dmit)_2]_2$ of the three following samples are the same, they were separately synthesized using $[Fe(C_5H_5)_2]BF_4$ [with the IR data (cm^{-1}) of ν(C=C) 1327.9w, 1288.1s; ν(C=S) and ν(C–S) 1057.2s, 1041.0s, 1022.3m, 994.6w], I_2–NaI [with the IR data (cm^{-1}) of ν(C=C) 1326.5w, 1287.3s; ν(C=S) and ν(C–S) 1056.7s, 1040.9s, 1021.9m, 993.9w] and TCNQ [with the IR data (cm^{-1}) of ν(C=C) 1327.3w, 1288.7m; ν(C=S) and ν(C–S) 1057.6s, 1041.3s, 1022.5m, 994.5w]. A crystal grown by using I_2–NaI was used for structural determination.

2.3 Structure determination

The X-ray diffraction data for $(Me_3NEt)_2[Pd(dmit)_2]$ and $(MeNEt_3)_2[Pd(dmit)_2]$ were collected on a Rigaku R-AXIS IIC area-detector diffractometer by the image-plate scans method, and those for $(NEt_4)_2[Pd(dmit)_2]$, $(Me_3NEt)[Pd(dmit)_2]_2$, $(MeNEt_3)[Pd(dmit)_2]_2$ and $(NEt_4)[Pd(dmit)_2]_2$ on a Bruker CCD area-detector diffractometer. Mo-Kα radiation (λ = 0.71073 Å) was used and the samples' temperatures were kept to 294 ± 1 K in all of the diffraction processes. By using SHELXL-97 programs, the structures were solved by direct methods and refined by full-matrix least-squares on F^2. Anisotropic displacement parameters were refined for all non-hydrogen atoms. See Table 1 for crystallographic data.

CCDC reference numbers 168855–168860.

See http://www.rsc.org/suppdata/dt/b1/b105854c/ for crystallographic data in CIF or other electronic format.

2.4 Electrical conductivity

The electrical conductivities of single crystals of $(Me_3NEt)[Pd(dmit)_2]_2$, $(MeNEt_3)[Pd(dmit)_2]_2$ and $(NEt_4)[Pd(dmit)_2]_2$ were measured by the conventional four-probe method. Taking a crystal of $(NEt_4)[Pd(dmit)_2]_2$ with dimensions of 1.2 × 0.25 × 0.02 mm^3, for example (other crystals are similar), four thin gold wires 0.02 mm in diameter were run parallel across the surface of the long platelet crystal and fixed in place using gold paste. The spacing between neighboring wires was 0.25 mm. The two wires in the middle (wire 2 and wire 3) were connected to a KEITHLEY-2001 digital voltmeter and the other two wires (wire 1 and wire 4) to a KEITHLEY-220 programmable current source. During the process of measurement (fixed or varying temperature), the electrical current was kept constant and low (typically 1 μA). The electrical resistivity (or conductivity) was obtained by Ohm's law. The room temperature conductivities are listed at the bottom of Table 1. The temperature was controlled using a Lakshore DRC-91CA temperature controller, which can decrease the temperature to 20 K, but in the natural warming process, the data above 40 K could only be reliably obtained owing to the limitations of the set-up. The resistivity–tempetature curves in cooling processes are shown in Fig. 1.

3 Results and discussion

3.1 Charge transfer in the process of synthesizing $Z[Pd(dmit)_2]_2$

Generally speaking, the process of the synthesis of conductive $Z[M(dmit)_2]_2$ is the process of charge transfer and then crystallization. Conductive Ni–dmit complexes were synthesized by successive charge transfer from non-conductive dianionic $[Ni(dmit)_2]^{2-}$ to non-conductive monoanionic $[Ni(dmit)_2]^{-}$ (by chemical oxidation) and then to conductive half-charged anionic $[Ni(dmit)_2]^{0.5-}$ (by electrochemical oxidation). By comparison, it seems impossible to isolate monoanionic complexes

Table 1 Crystal data of a series of $Z_2[M(dmit)_2]$ and a series of $Z[M(dmit)_2]_2$

Compound	$(Me_3NEt)_2$[-Pd(dmit)$_2$]	$(MeNEt_3)_2$-[Pd(dmit)$_2$]	$(NEt_4)_2$-[Pd(dmit)$_2$]	(Me_3NEt)-[Pd(dmit)$_2]_2$	$(MeNEt_3)$-[Pd(dmit)$_2]_2$	(NEt_4)[Pd(dmit)$_2]_2$
Formula	$C_{16}H_{28}N_2PdS_{10}$	$C_{20}H_{36}N_2PdS_{10}$	$C_{22}H_{40}N_2PdS_{10}$	$C_{17}H_{14}NPd_2S_{20}$	$C_{19}H_{18}NPd_2S_{20}$	$C_{20}H_{20}NPd_2S_{20}$
Formula weight	675.49	731.60	759.65	1086.46	1114.52	1128.55
Crystal system	Monoclinic	Orthorhombic	Orthorhombic	Monoclinic	Triclinic	Triclinic
Space group	$P2_1/c$	*Pbca*	*Pccn*	$P2_1/m$	$P1$	$P\bar{1}$
Absorption coefficient/mm^{-1}	1.432	1.263	1.171	2.346	2.274	2.215
Crystal size/mm	0.32 × 0.30 × 0.03	0.50 × 0.30 × 0.08	0.27 × 0.20 × 0.08	0.08 × 0.08 × 0.02	0.12 × 0.08 × 0.02	0.27 × 0.11 × 0.03
a/Å	11.471(2)	10.410(3)	11.805(2)	6.2647(5)	6.222(3)	6.297(1)
b/Å	10.522 (4)	12.937(5)	13.477(3)	36.486 (3)	7.838(5)	7.875(1)
c/Å	12.358 (2)	23.445(2)	21.458(4)	7.7255(6)	18.622(2)	18.885(3)
α/°					84.98(1)	83.95(1)
β/°	111.76(3)			108.976(3)	83.70(1)	83.30(1)
γ/°					73.13(1)	72.74(1)
Cell volume/Å^3, *Z*	1385.3(5), 2	3157.4(11), 4	3414.0(12), 4	1669.9(2), 2	862.2(6), 1	885.8(3), 1
Calculated density/g cm^{-3}	1.619	1.539	1.478	2.160	2.146	2.115
Measured reflections	2047	8289	22434	3873	4543	4364
Independent reflections	2047	2746	4216	3861	4471	4364
θ range/°	1.91 to 24.99	2.62 to 25.46	1.90 to 28.31	2.79 to 27.53	2.20 to 27.67	2.18 to 28.38
Site symmetry of anion	$\bar{1}$	$\bar{1}$	$\bar{1}$	1	1	1
Site symmetry of cation	1 (ordered)	1 (ordered)	2 (one ordered, one disordered)	*m* (disordered)	1 (ordered)	$\bar{1}$ (disordered)
R_{int}	0.000	0.0442	0.0566	0.000	0.0000	0.0000
Final *R* indices [$I > 2\sigma(I)$] *R*, *wR*	0.0668, 0.1856	0.0567, 0.1360	0.0582, 0.1614	0.0404, 0.0989	0.0945, 0.2229	0.0779, 0.1844
Conductivity at 300 K/Ω^{-1} cm^{-1}				58 [at a direction on (010) plane]	5.0 [at a direction on (001) plane]	2.2 {at [001] direction on (001) plane}
Activation energy/eV				0.056 (at 300–80 K), 0.02 (at 55–40 K)	0.041 (at 140–35 K)	0.036 (at 300–45 K)

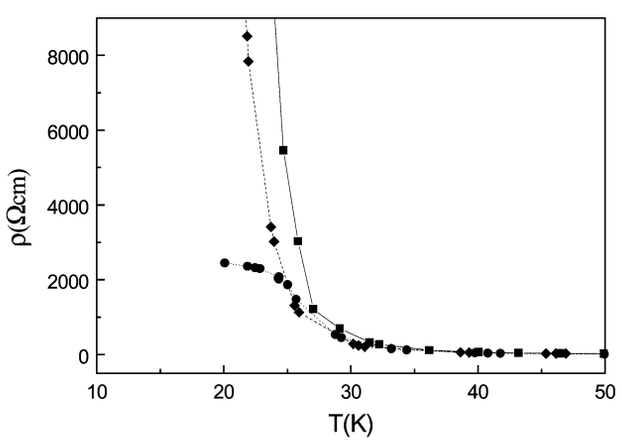

Fig. 1 Resistivity–temperature curves (cooling process) of (Me_3NEt)-$[Pd(dmit)_2]_2$ (●), $(MeNEt_3)[Pd(dmit)_2]_2$ (■) and $(NEt_4)[Pd(dmit)_2]_2$ (◆).

of $Z[Pd(dmit)_2]$ by the reaction of dianionic $Z_2[Pd(dmit)_2]$ with oxidation agents, such as I_2–NaI, which we had once used to synthesize and isolate monoanionic Ni–dmit complexes. The monoanionic $[Pd(dmit)_2]^-$ may be an unstable intermediate which quickly loses "half an electron" under the further attack of the acceptor and forms half-charged $[Pd(dmit)_2]^{0.5-}$. More exactly, two $[Pd(dmit)_2]^-$ anions may form the dimer $[Pd(dmit)_2]_2^{2-}$ and the dimer jointly transfers an electron to the acceptor. It have been proved by crystallographic determination and supported by theoretical calculation [13] that metal dithiolene complexes of Pd have a strong tendency to form dimers.

The half-charged anionic conducting crystals $Z[M(dmit)]_2$ are usually prepared by the electrochemical oxidation method. Our experiment proves that crystals of $(Me_3NEt)[Pd(dmit)_2]_2$, $(MeNEt_3)[Pd(dmit)_2]_2$ and $(Et_4N)[Pd(dmit)_2]_2$ can be smoothly synthesized by chemical oxidation using a variety of electron acceptor, such as I_2–NaI, TCNE, TCNQ and $[Fe(C_5H_5)_2]BF_4$. The successful preparation of a series of $Z[Pd(dmit)]_2$ crystals may be because of the simplicity of the following primary physicochemical process.

$$2[Pd(dmit)_2]^- \text{ (pre-dimer)} + \text{acceptor} \longrightarrow [Pd(dmit)_2]_2^- \text{ (dimer)} + [\text{acceptor}]^- \quad (1)$$

3.2 Semiconductor behavior and the potential to conduct

All of the three title conducting complexes are typical semiconductors; the curves of the natural logarithm of conductivity $\ln(\sigma)$ *versus* the inverse of temperature T^{-1}, shown in Fig. 2, are quite good straight lines with negative slopes. The activation energies, obtained from the slopes of the fitted straight lines and listed at the bottom of Table 1, are of the order of 0.05eV, indicating the very narrow band gaps of these crystals. Among the three curves in Fig. 2, the curve of $(NEt_4)[Pd(dmit)_2]_2$ shows the best linearity, with a linear factor *R* of 0.99932 at the widest temperature range (300–45 K). We also performed a linear fit of $\ln(\sigma)$–$T^{-1/2}$, but the linearity is unsatisfactory, with an *R* factor of only 0.99234 at the same temperature range, the result is different from the reported $\ln(\sigma)$–$T^{-1/2}$ linear relationship of $(NEt_4)[Pd(dmit)_2]_2$.[10,14] This difference may be caused by the four-probe measuring method employed here and the two-probe method used in the previous reports.

The conductivity of $(Me_3NEt)[Pd(dmit)_2]_2$ shows several features. (1) The conductivity at room temperature of this complex is one order of magnitude larger than that of its two analogues (see Table 1). (2) Below 55 K, its $\ln(\sigma)$–T^{-1} curve becomes flat and the activation energy reduces (less than 0.02eV in the range 55–40 K) as shown in Fig. 2. (3) The most meaningful feature shown in Fig. 1 is that the slope of the ρ–T curve of $(Me_3NEt)[Pd(dmit)_2]_2$ shows a tendency to become smaller

Table 2 Mean bond lengths of various types and deviations from least-squares planes (Å)

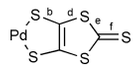

	Pd–S	b-Type S–C	C=C	d-Type S–C	e-Type S–C	f-Type S–C	Average S–C	Deviation from plane[a]	Plane-bending[b]
$(Me_3NEt)_2[Pd(dmit)_2]$	2.3173(9)	1.736(3)	1.372(4)	1.748(3)	1.722(3)	1.675(3)	1.726(3)	0.052(2)	0.000(1)
$(Me_3NEt)[Pd(dmit)_2]_2$	2.3024(5)	1.699(2)	1.375(2)	1.748(2)	1.726(2)	1.652(2)	1.714(2)	0.094(1)	0.186(1)
$(MeNEt_3)_2[Pd(dmit)_2]$	2.314(2)	1.730(5)	1.356(7)	1.749(5)	1.721(6)	1.663(5)	1.723(5)	0.020(2)	0.000(1)
$(MeNEt_3)[Pd(dmit)_2]_2$	2.292(1)	1.700(4)	1.348(5)	1.760(4)	1.749(5)	1.630(5)	1.721(5)	0.103(2)[c]	0.190(1)[d]
$(NEt_4)_2[Pd(dmit)_2]$	2.319(2)	1.742(6)	1.345(8)	1.745(6)	1.726(7)	1.656(7)	1.726(7)	0.051(3)	0.000(1)
$(NEt_4)[Pd(dmit)_2]_2$	2.300(1)	1.695(3)	1.376(5)	1.742(3)	1.727(4)	1.646(4)	1.710(4)	0.102(2)	0.205(1)

[a] The mean deviation from the least-squares plane obtained from all 17 atoms of the anion. [b] Defined by the deviation of Pd from the least-squares plane obtained from 17 atoms of the anion. [c] Average of the measuements for the two independent anions [0.0777(2) and 0.1234(2) Å]. [d] Average of the measuements for the two independent anions [0.166(1) and 0.213(1) Å].

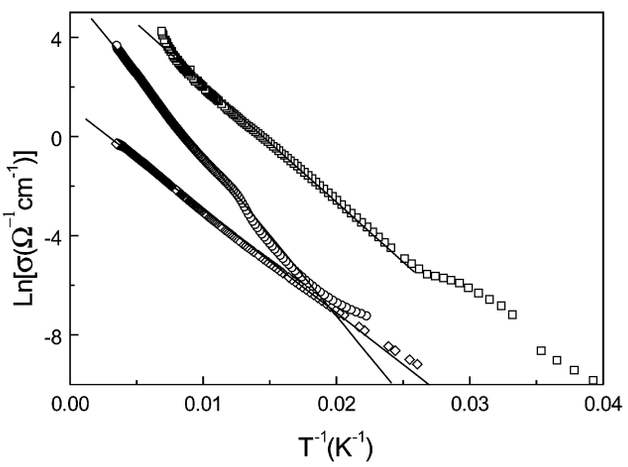

Fig. 2 The curves (warming process) of the natural logarithm of conductivity ln(σ) *versus* the inverse of temperature T^{-1} for $(Me_3NEt)[Pd(dmit)_2]_2$ (○ middle line), $(MeNEt_3)[Pd(dmit)_2]_2$ (□ upper line) and $(NEt_4)[Pd(dmit)_2]_2$ (◇ lower line).

and smaller below 25 K. We expected the slope would eventually become negative, but unfortunately we failed to obtain data below 20 K because of the limitations of our set-up. Although evidence of the expected semiconductor ⟶ conductor transformation did not emerge, the phase transformation may occur under fairly high pressure since the size of the cation $(Me_3NEt)^+$ falls just between the size of $(Me_4N)^+$ and $(Me_2NEt_2)^+$, while both α-$(Me_4N)[Pd(dmit)_2]_2$ and $(Me_2NEt_2)[Pd(dmit)_2]_2$ have been reported to be superconductors at 6.2 (6.5) and 4 K (2.4 kbar), respectively.[5,6]

3.3 Structures of $(Me_3NEt)[Pd(dmit)_2]_2$, $(MeNEt_3)[Pd(dmit)_2]_2$ and $(NEt_4)[Pd(dmit)_2]_2$

3.3.1 Planar and conjugated molecular configuration of $[Pd(dmit)_2]^{2-}$ and $[Pd(dmit)_2]^{0.5-}$. The anions of the six title complexes adopt a planar configuration with quite a high degree of conjugation (all C–C and C–S bond lengths are intermediate between single and double bonds). This feature is shown in all the molecular packing diagrams below and in Table 2. Statistical averages over the six title complexes and over all their bonds shows that when $[Pd(dmit)_2]^{2-}$ is oxidized to $[Pd(dmit)_2]^{0.5-}$, the Pd–S bonds and b-type of S–C bonds (shown in Table 2) are shortened by 0.019 and 0.04 Å, respectively, while the C=C bond is stretched by 0.009 Å and the lengths of the other types of S–C bonds in the external five-membered rings remain constant. This means that $[Pd(dmit)_2]^{0.5-}$ has more conjugation compared to its $[Pd(dmit)_2]^{2-}$ precursor and also seems to imply that the charge transfer of $[Pd(dmit)_2]^{2-}$ mainly takes place at its Pd-containing five-membered rings.

The planarity of $[Pd(dmit)_2]^{0.5-}$ is not as good as its $[Pd(dmit)_2]^{2-}$ precursor, as shown in the last two columns of Table 2. This is because of the condensed packing of $[Pd(dmit)_2]^{0.5-}$ and its strong dimeric nature, which has the result of the bending the molecular plane of $[Pd(dmit)_2]^{0.5-}$ in its conducting complexes. The degree of plane bending can be scaled by looking at the deviation of Pd from the least-squares plane, shown in Table 2.

3.3.2 Packing style of $(Me_3NEt)[Pd(dmit)_2]_2$, $(MeNEt_3)[Pd(dmit)_2]_2$ and $(NEt_4)[Pd(dmit)_2]_2$. $(Me_3NEt)[Pd(dmit)_2]_2$, $(MeNEt_3)[Pd(dmit)_2]_2$ and $(NEt_4)[Pd(dmit)_2]_2$ crystallize in the $P2_1/m$, $P\bar{1}$ and $P\bar{1}$ space groups, respectively, while their packing styles basically belong to the same structural motif with the following features. (1) The $[Pd(dmit)_2]^{0.5-}$ anions are strongly and vertically linked, forming face-to-face eclipsed dimers (see Fig. 3–5). These dimers are then weakly linked (also in a face-to-face manner) to form columns or stacks along a definite direction {*c*-direction in $(Me_3NEt)[Pd(dmit)_2]_2$ and *b*-direction for $(MeNEt_3)[Pd(dmit)_2]_2$ and $(NEt_4)[Pd(dmit)_2]_2$} (see Fig. 3–5

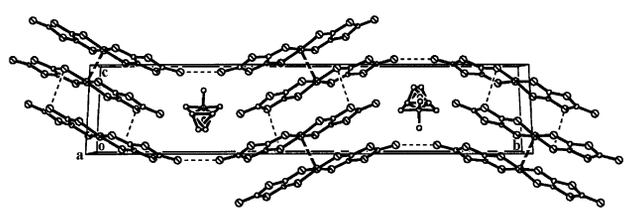

Fig. 3 View along the *a*-axis of the $(Me_3NEt)[Pd(dmit)_2]_2$ crystal; $(Me_3NEt)^+$ is disordered.

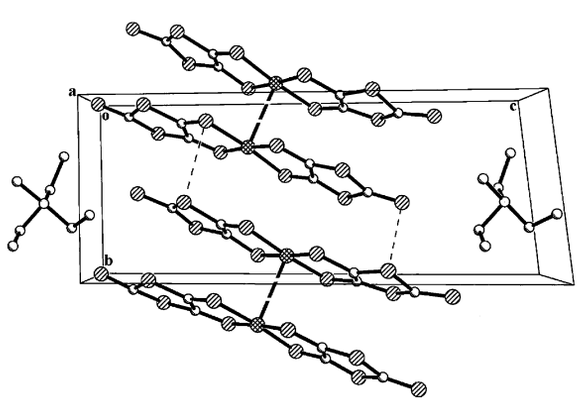

Fig. 4 View along the *a**-axis of $(MeNEt_3)[Pd(dmit)_2]_2$.

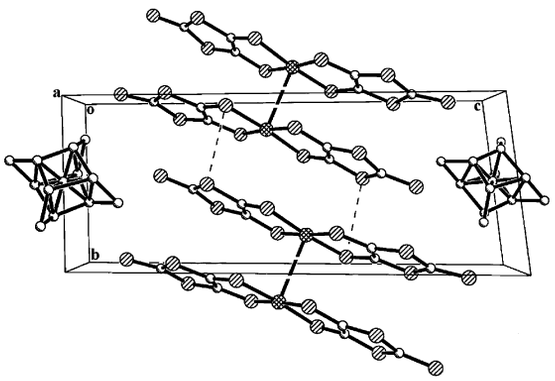

Fig. 5 View along the a^*-axis of $(NEt_4)[Pd(dmit)_2]_2$; $(NEt_4)^+$ is disordered.

Fig. 6 Platelet-shaped crystals of $(NEt_4)[Pd(dmit)_2]_2$ (left) and fiber-shaped crystals of "$(PrNEt_3)[Pd(dmit)_2]_2$" (right). $(Me_3NEt)[Pd(dmit)_2]_2$ and $(MeNEt_4)[Pd(dmit)_2]_2$ have the same crystalline habits as $(NEt_4)[Pd(dmit)_2]_2$.

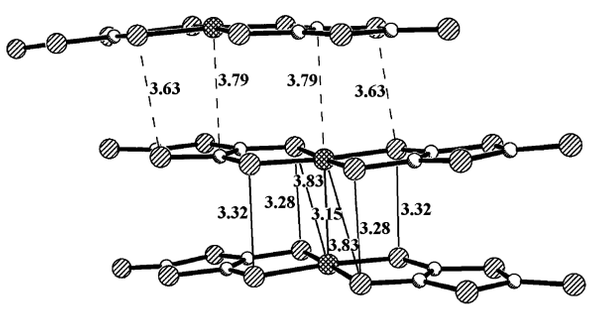

Fig. 7 Structure of the molecular column of $(Me_3NEt)[Pd(dmit)_2]_2$ showing the face-to-face eclipsed dimer.

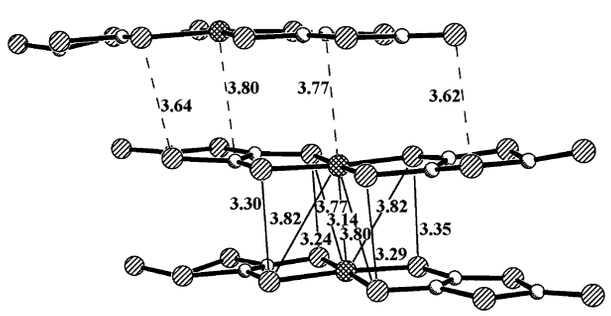

Fig. 8 Structure of $(MeNEt_3)[Pd(dmit)_2]_2$ showing the two molecular planes in a dimer bent away from each other.

and 7–9). (2) There are many strong transverse side-by-side S ··· S intermolecular contacts between neighboring $[Pd(dmit)_2]^{0.5-}$ groups; these transverse and vertical intermolecular interactions lead to a kind of two-dimensional anionic sheet (see Fig. 10–13). Projected along the long axis of $[Pd(dmit)_2]^{0.5-}$, this sheet shows a two-dimensional quasi-centred rectangular lattice (see Fig. 10). (3) The neighboring anionic

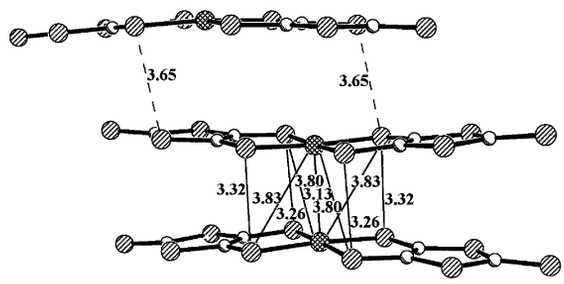

Fig. 9 Structure of $(NEt_4)[Pd(dmit)_2]_2$ showing the strong and weak bonding within and between the dimers.

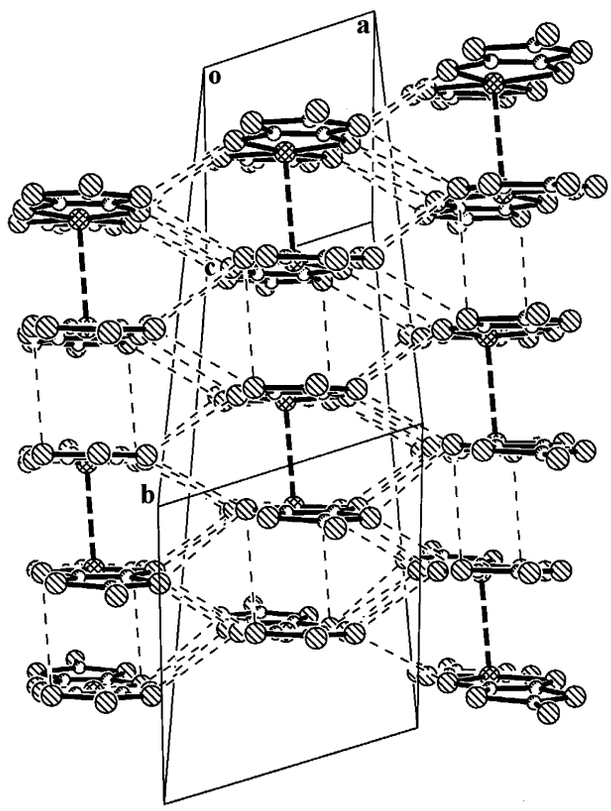

Fig. 10 View along the long axis of $[Pd(dmit)_2]^{0.5-}$ and the two-dimensional quasi-centred rectangular lattice of $(Me_3NEt)[Pd(dmit)_2]_2$.

sheets are sandwiched by sheets of ordered {in the case $(MeNEt_3)[Pd(dmit)_2]_2$} or disordered cations (see Fig. 3–5). The stoichiometric ratio of cations to anions is 1 : 2.

The same structural motif is found in $(Me_2NEt_2)[Pd(dmit)_2]_2$[6] {which is isostructural with $(NEt_4)[Pd(dmit)_2]_2$), α-$(Me_4N)[Pd(dmit)_2]_2$,[15] β-$(Me_4N)[Pd(dmit)_2]_2$,[5] $(Me_4P)[Pd(dmit)_2]_2$[7] and $(Me_4As)[Pd(dmit)_2]_2$[15]}. Since the size of cation is the variable with which the anionic structure can be tuned, a certain critical cation size $(R_nNR'_{4-n})^+$ must exist, with which the structure of the corresponding conductive complex is kept from the above motif. We have tried to synthesize $(PrNEt_3)[Pd(dmit)_2]_2$, but only obtained fibre-shaped crystals (Fig. 6) which were unsuitable for X-ray structure analysis. The structure of this complex must be different from the title complexes, judging by its very different crystalline habits. Therefore, the critical size can be practically regarded as the size of $(NEt_4)^+$.

3.3.3 The face-to-face eclipsed dimers and the one-dimensionality of the columns. As shown in Table 3 and in Fig. 7–9, many quasi-bonds exist between the two near planar PdS_4 moieties in the dimers. The Pd–Pd distances in the dimers of

Table 3 Face-to-face intermolecular distances within and between the dimers (Å)[a]

Compound		$(Me_3NEt)[Pd(dmit)_2]_2$	$(MeNEt_3)[Pd(dmit)_2]_2$	$(NEt_4)[Pd(dmit)_2]_2$
Intra-dimer	Pd–Pd	3.1511(3)	3.1440(16)	3.1293(6)
	S ⋯ S	2 × 3.2780(7), 2 × 3.3233(7)	3.238(2), 3.286(2), 3.300(2), 3.349(2)	2 × 3.2596(14), 2 × 3.3159(14)
	Mean S ⋯ S	3.301(1)	3.293(2)	3.288(1)
	Pd ⋯ S	2 × 3.835(1)	3.766(2), 3.822(2), 3.823(2), 3.802(2)	2 × 3.795(1), 2 × 3.828(1)
	Mean Pd ⋯ S		3.803(2)	3.811(1)
Inter-dimer	S ⋯ S	2 × 3.634(1),	3.620(2), 3.638(2)	2 × 3.648(1)
	Pd ⋯ C	2 × 3.788(1)	3.774(2), 3.795(2)	
Spacing in dimer D_1		3.511	3.496	3.517
Spacing between dimers D_2		3.562	3.552	3.555
$D_2 - D_1$		0.049	0.056	0.038
Pd–Pd distance in dimer R_1		3.1511(3)	3.1440(16)	3.1293(6)
Pd–Pd distance between dimers R_2		5.093(1)	5.212(1)	5.296(1)
$R_2 - R_1$		1.942	2.068	2.167

[a] van der Waals radii: Pd–Pd = 4.6, S–S = 3.7, Pd–S = 4.15, Pd–C = 4.00 Å.

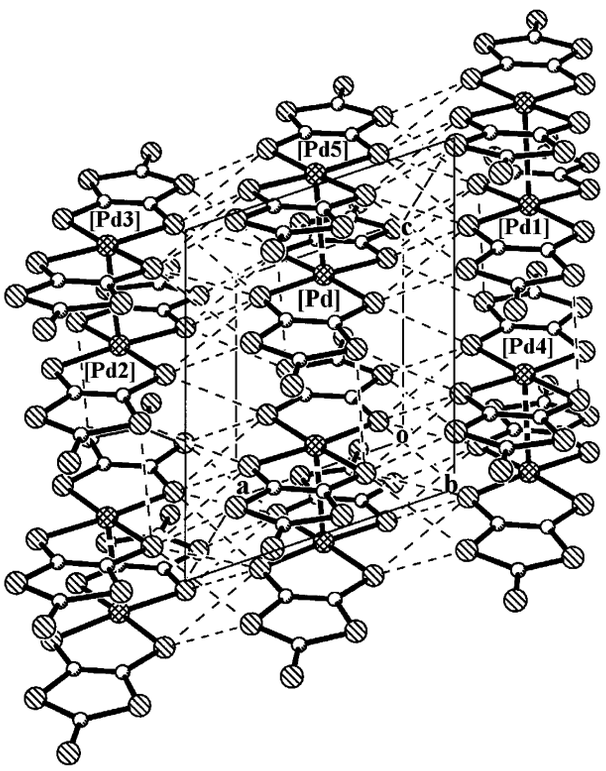

Fig. 11 View along the *b*-axis of $(Me_3NEt)[Pd(dmit)_2]_2$.

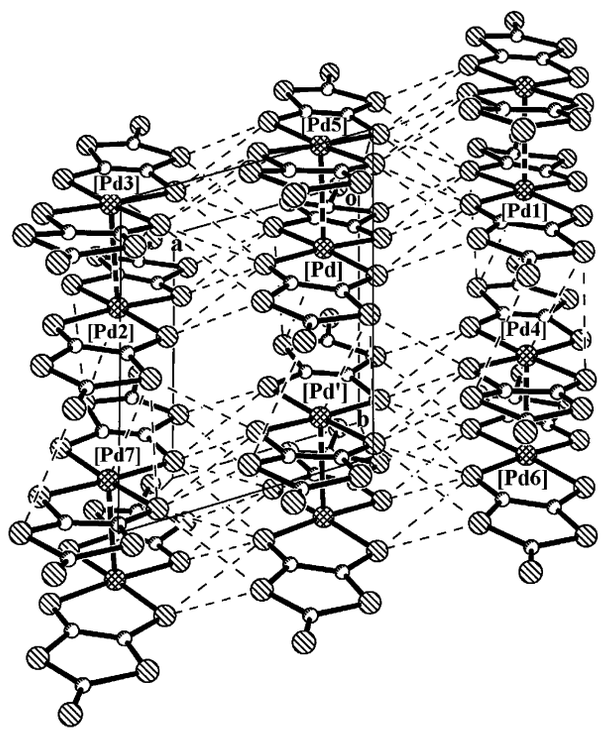

Fig. 12 View along the *c**-axis of $(MeNEt_3)[Pd(dmit)_2]_2$.

$(Me_3NEt)[Pd(dmit)_2]_2$, $(MeNEt_3)[Pd(dmit)_2]_2$ and $(NEt_4)[Pd(dmit)_2]_2$ are 3.150(1), 3.144(2) and 3.129(1) Å, respectively, so the Pd–Pd unit can be regarded as being covalently bonded. There are also four S ⋯ S connections in the dimers of $(Me_3NEt)[Pd(dmit)_2]_2$, $(MeNEt_3)[Pd(dmit)_2]_2$ and $(NEt_4)[Pd(dmit)_2]_2$, with average distances of 3.301(1), 3.293(2) and 3.288(1) Å, respectively. There are two equivalent Pd ⋯ S interactions in $(Me_3NEt)[Pd(dmit)_2]_2$ with distances of 3.833(1) Å, while the number of the Pd ⋯ S contacts in $(MeNEt_3)[Pd(dmit)_2]_2$ and $(NEt_4)[Pd(dmit)_2]_2$ is four, with average distances of 3.803(2) and 3.811(1) Å, respectively. So the face-to-face π–π intra-dimer intermolecular interactions are very strong (compare all the above intermolecular distances with the sum of the van de Waals radii: Pd ⋯ Pd = 4.60 Å, S ⋯ S = 3.70 Å and Pd ⋯ S = 4.15 Å) and the strength of these intra-dimer interactions gives the sequence $(Me_3NEt)[Pd(dmit)_2]_2$ < $(MeNEt_3)[Pd(dmit)_2]_2$ ~ $(NEt_4)[Pd(dmit)_2]_2$. This is in accordance with the sequence of plane deviation and the plane bending shown in the last two columns in Table 2.

In considering the strength of the face-to-face inter-dimer interactions, Table 3 and Fig. 7–9 show the sequence $(Me_3NEt)[Pd(dmit)_2]_2$ ~ $(MeNEt_3)[Pd(dmit)_2]_2$ > $(NEt_4)[Pd(dmit)_2]_2$. Among the above three complexes, $(Me_3NEt)[Pd(dmit)_2]_2$ has the weakest intra-dimer bonding and the strongest inter-dimer interactions. So the conjugacy or the uniformity of the molecular column of $(Me_3NEt)[Pd(dmit)_2]_2$ is comparatively the best. Although the one-dimensionality of the molecular column of $(Me_3NEt)[Pd(dmit)_2]_2$ is by no means satisfactory, its better than that of $(MeNEt_3)[Pd(dmit)_2]_2$ and $(NEt_4)[Pd(dmit)_2]_2$. This conclusion is be supported by the difference between R_2 and R_1 ($R_2 - R_1$), shown in Table 3, where R_2 is the inter-dimer Pd ⋯ Pd distance and R_1 the intra-dimer Pd–Pd distance. The better the one-dimensionality of the molecular column, the smaller $R_2 - R_1$ is. From the last line of Table 3, we believe that the face-to-face one-dimensionality has the sequence $(Me_3NEt)[Pd(dmit)_2]_2$ > $(MeNEt_3)[Pd(dmit)_2]_2$ > $(NEt_4)[Pd(dmit)_2]_2$.

It might be supposed that the uniformity of the spacing between the molecular planes may be also a measure for the

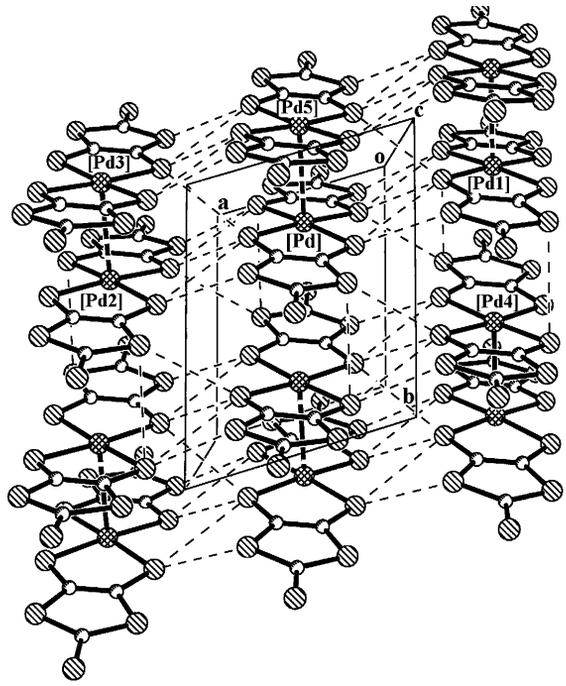

Fig. 13 View along the c^*-axis of $(NEt_4)[Pd(dmit)_2]_2$.

one-dimensionality. However, the differences $(D_2 - D_1)$ between the inter-dimer spacing (D_2) and the intra-dimer spacing (D_1) is small. This can also be understood by considering the dimerization (see Table 3). The bonding of two PdS_4 moieties makes the two faces of the dimer bend away from each other and makes the plane-to-plane spacings, which are calculated based on least-squares procedures, much larger than the Pd–Pd distances in the dimer (see Fig. 7–9 and Table 3).

3.3.4 The transverse side-by-side S ··· S intermolecular interactions in the anionic sheet. As shown in Fig. 10–13, each anion [Pd] {[Pd] is used as an abbreviation for $[Pd(dmit)_2]^{0.5-}$ hereafter} has six nearest neighbors. Two of the six are face-to-face arranged, one is strongly linked to [Pd] and the other is weakly linked to it. The other four neighbors ($[Pd_1]$, $[Pd_2]$, $[Pd_3]$ and $[Pd_4]$) are side-by-side linked to the central [Pd] by many S ··· S intermolecular interactions with "bond lengths" considerably shorter than the sum of the van der Waals radii. If this S ··· S intermolecular interaction can be temporarily considered a bond, the total side-by-side bond number of a [Pd] in $(Me_3NEt)[Pd(dmit)_2]_2$ is 18, with an average length of 3.5475(8) Å, that of $(MeNEt_3)[Pd(dmit)_2]_2$ and $(NEt_4)[Pd(dmit)_2]_2$ are 16 [average length 3.545(2)] and 13 [average length 3.5495(14) Å], respectively. As shown in Table 4, the strength of the side-by-side S ··· S intermolecular interactions obviously have the sequence $(Me_3NEt)[Pd(dmit)_2]_2$ > $(MeNEt_3)[Pd(dmit)_2]_2$ > $(NEt_4)[Pd(dmit)_2]_2$.

The above sequence also applies to the two-dimensionality by the following reasoning. As shown in Table 4 and Fig. 10–13, there are four groups of side-by-side S ··· S intermolecular linkages corresponding to the four side-by-side neighbors of a [Pd]. If one or two groups of these linkages are too weak, the two-dimensionality of the anionic sheet will be lost. In $(NEt_4)[Pd(dmit)_2]_2$ (see Fig. 13 and Table 4), the linkage (by five S ··· S bonds) of [Pd] with its left $[Pd_2]$ and right $[Pd_1]$ neighbours forms a one-dimensional ··· $[Pd_2]$ ··· [Pd] ··· [Pd1] ··· chain along the *a*-axis, the periodicity of the chain is just the length of *a*, and two chains are dimerized. In $(MeNEt_3)[Pd(dmit)_2]_2$ (see Fig. 12 and Table 4), the same *a*-directional double chain exists and it is further strengthened by the strong third side-by-side linkage [Pd] ··· $[Pd_3]$. In $(Me_3NEt)[Pd(dmit)_2]_2$, in addition to the one-dimensional double chain, the two-dimensionality becomes noticeable through: (1) the much stronger fourth side-by-side linkage [Pd] ··· $[Pd_4]$ and (2) the better one-dimensionality of its face-to-face column.

3.3.5 Calculated band structures. In order to further reveal the structure dependence of the conductivity, tight-binding band calculations have been carried out for $(Me_3NEt)[Pd(dmit)_2]_2$ and $(NEt_4)[Pd(dmit)_2]_2$ based on the extended Hückel molecular orbital (EHMO) method using Slater-type atomic orbitals.[13] The calculation object in the two-dimensional band calculation is the dimer [Pd]–$[Pd_5]$, and the two translation vectors are lattice bases *a* and *c* for $(Me_3NEt)[Pd(dmit)_2]_2$, and *a* and *b* for $(NEt_4)[Pd(dmit)_2]_2$ (see Fig. 11 and 13). Only the nearest neighbors have been taken into account in the band calculation and the results are shown in Fig. 14 and 15.

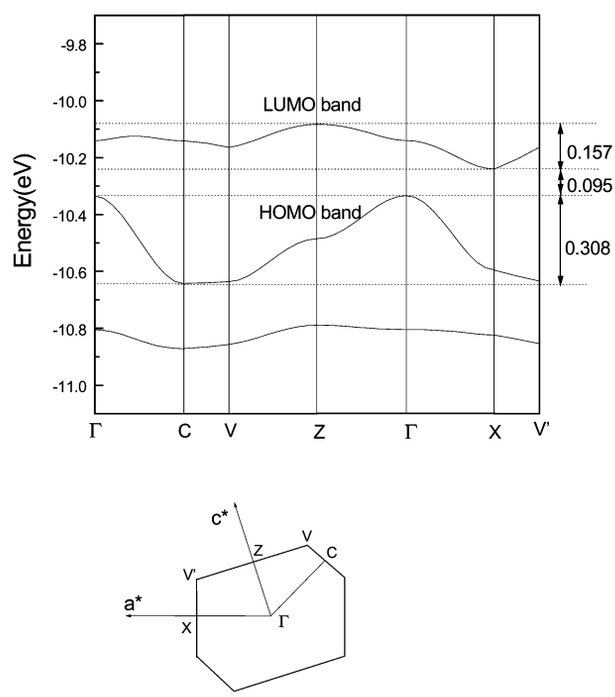

Fig. 14 Tight-binding band structure and the Brillouin zone of $(Me_3NEt)[Pd(dmit)_2]_2$.

Fig. 14 shows that the HOMO band width E_H, the energy gap between the HOMO and LUMO bands E_g, and the LUMO band width E_L of $(Me_3NEt)[Pd(dmit)_2]_2$ are 0.308, 0.095 and 0.157 eV, respectively. For $(NEt_4)[Pd(dmit)_2]_2$, E_H = 0.306, E_g = 0.150 and E_L = 0.094 eV. Compared with $(NEt_4)[Pd(dmit)_2]_2$, $(Me_3NEt)[Pd(dmit)_2]_2$ obviously has a wider LUMO band and a narrower gap, so it has a more favorable band structure for conductivity.

3.3.6 Brief discussion of structure–conductivity relationships. The platelet crystals are too small and too thin to have their planes indexed by the X-ray method. However, the surface of the platelet crystals, *i.e.* the cleavage face of the crystal, can be reasonably assigned to be the crystallographic (010) plane for $(Me_3NEt)[Pd(dmit)_2]_2$ (see Fig. 11) and the (001) plane for the other two crystals (see Fig. 12 and 13) because this kind of plane is the anionic sheet with more or less two-dimensional character. Hence, the data shown at the bottom of Table 1 are the conductivities along a direction on above the plane and the phrase "resistivity (or conductivity) of the plane" is defined in this way. Furthermore, the as-measured conductivity (2.2 Ω^{-1} cm^{-1}) of $(NEt_4)[Pd(dmit)_2]_2$ can be supposed to be the conductivity along the *a*-axis direction, which is the direction

Table 4 The transverse side-by-side S ··· S intermolecular distances (Å) in the anionic sheet

Anion pair[a]	$(Me_3NEt)[Pd(dmit)_2]_2$	$(MeNEt_3)[Pd(dmit)_2]_2$ (Two independent anions)		$(NEt_4)[Pd(dmit)_2]_2$
[Pd] ··· [Pd_1]	3.5852(7), 3.5168(7), 3.4661(7), 3.5106(7), 3.5408(7)	3.579(2), 3.508(2), 3.488(2), 3.504(2), 3.563(2)	3.500(2), 3.509(2), 3.419(2), 3.502(2), 3.522(2) ([Pd′] ··· [Pd_4])	3.5562(15), 3.5180(14), 3.4640(14), 3.5335(14), 3.5656(14)
[Pd] ··· [Pd_2]	3.5852(7), 3.5168(7), 3.4661(7), 3.5106(7), 3.5408(7)	3.579(2), 3.508(2), 3.488(2), 3.504(2), 3.563(2)	3.500(2), 3.509(2), 3.419(2), 3.502(2), 3.522(2) ([Pd′] ··· [Pd_7])	3.5562(15), 3.5180(14), 3.4640(14), 3.5335(14), 3.5656(14)
[Pd] ··· [Pd_3]	3.5738(7), 3.5750(7), 3.4820(7), 3.5737(7), 3.5737(7)	3.652(2), 3.559(2), 3.548(2), 3.613(2), 3.651(2)	3.593(2) ([Pd′] ··· [Pd_2])	3.6465(14)
[Pd] ··· [Pd_4]	3.5779(8), 3.6130(7), 3.5779(8)	3.593(2)	3.652(2), 3.559(2), 3.548(2), 3.613(2), 3.651(2) ([Pd′] ··· [Pd_6])	3.6115(14), 3.6115(14)
Total S ··· S bonds	18	16	16	13
Average	3.5437(8)	3.545(2)		3.5495(14)

[a] The anion $[Pd(dmit)_2]^{0.5-}$ is abbreviated to [Pd], the data are the S ··· S distances between anionic pairs.

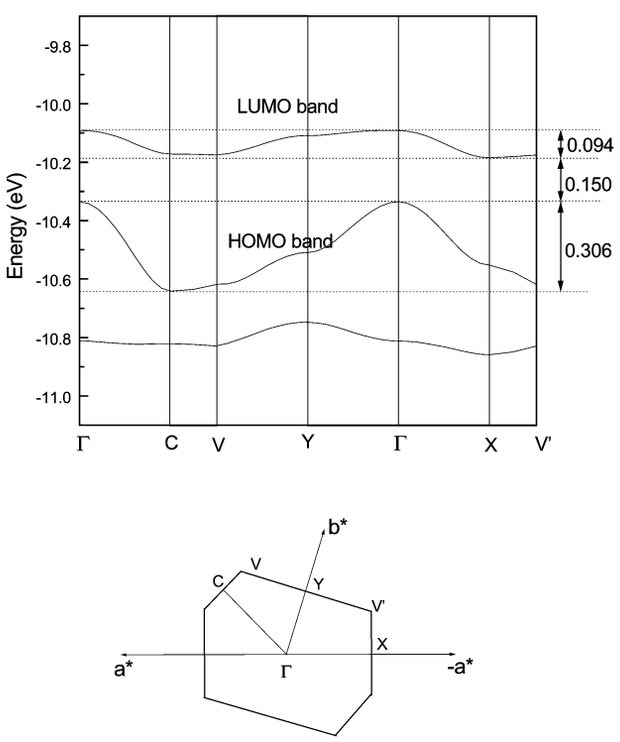

Fig. 15 Tight-binding band structure and the Brillouin zone of $(NEt_4)[Pd(dmit)_2]_2$.

of the side-by-side double chain shown in Fig. 13, because this platelet could be further cleaved to a long platelet-bar and the electrical current was just along the longest dimension of the 1.2 × 0.25 × 0.02 mm^3 $(NEt_4)[Pd(dmit)_2]_2$ sample. Therefore, the conductivity of 2.2 Ω^{-1} cm^{-1} is the maximum among various directions on the (001) plane of the crystal and so the conductivities of the three title complexes must fall in the sequence $(Me_3NEt)[Pd(dmit)_2]_2$ > $(MeNEt_3)[Pd(dmit)_2]_2$ > $(NEt_4)[Pd(dmit)_2]_2$.

This sequence is agreement with the sequence of the strength of the side-by-side S ··· S interactions of above complexes. The two-dimensionality obviously plays a key role in the conductivity. The evolution of the resistivity–temperature curve of $(Me_3NEt)[Pd(dmit)_2]_2$, shown in Fig. 1, may also be closely related to the evolution of the two-dimensionality.

4 Conclusions

In order to explore the influence of cation size on the structure and conductivity properties, we have synthesized a series of half-charged anionic conducting crystals $Z[Pd(dmit)_2]_2$ [Z = $(Me_3NEt)^+$, $(MeNEt_3)^+$, $(NEt_4)^+$] from dianionic $Z_2[Pd(dmit)_2]$ and have determined their structures. We have developed a smooth synthesis and crystallization method and our experiments reveal that monoanionic $Z[Pd(dmit)_2]$ cannot be obtained because of the intense dimerization tendency of this kind of conductive Pd complex. Single crystals of the three title complexes show quite high conductivity at room temperature and their resistivity–temperature curves exhibit semiconductor behavior with very narrow gaps. Basically, these three complexes show a one-dimensional double chain structure based on the linkage of strong uniform side-by-side S ··· S interactions and strong face-to-face intra-dimer interactions (see Fig. 11–13). There are also some S ··· S intermolecular interactions between the double chains which endow the anionic sheet with some two-dimensional character (see Fig. 11–13). The greater the two-dimentional character of a structure, the better its conductivity, such as in the case of $(Me_3NEt)[Pd(dmit)_2]$. We have proven that when the size of the cation Z in $Z[Pd(dmit)_2]_2$ is finely tuned carbon-by-carbon [$(Me_4N)^+$ ⟶ $(Me_3NEt)^+$ ⟶ $(Me_2NEt_2)^+$ ⟶ $(MeNEt_3)^+$ ⟶ $(NEt_4)^+$], the resulting molecular conductors belong to the same structure motif, as shown in Fig. 10. If the cation size is larger than the critical size of $(NEt_4)^+$, the corresponding complex may no longer belong to this structure motif and, hence it is quite impossible for it to display superconductivity. In searching for new superconductors in the Pd–dmit complex family, the use of small cations seems to provide the most promise. As a stuctural criterion, the ideal

two-dimensional anionic sheet should have four groups with equally strong side-by-side S ··· S intermolecular linkages, corresponding to the four side-by-side neighbors of the [Pd(dmit)]$^{0.5-}$ anion. The uniformity of the face-to-face intermolecular interactions between the two upper and lower neighbors of the [Pd(dmit)]$^{0.5-}$ is also critical. Dimerization in the face-to-face direction, if unavoidable, may be reduced at low temperature and high pressure in a superconductor of this kind. Among others, $(Me_3NEt)[Pd(dmit)_2]_2$ shows the possibility of becoming a superconductor under fairly high pressure, since the size of its cation $(Me_3NEt)^+$ is just between $(Me_4N)^+$ and $(Me_2NEt_2)^+$ in terms of size, and both α-(Me_4N)-$[Pd(dmit)_2]_2$ and $(Me_2NEt_2)[Pd(dmit)_2]_2$ have been reported to be superconductors.[5,6]

Acknowledgements

This work was supported by the National Natural Science Foundation of China (no. 20172034 and 29672023), the State Key Program of China and by a Hong Kong Research Grant, earmarked grant CUHK 4022/98P.

References

1 M. Bousseau, L. Valade, J.-P. Legros, P. Cassoux, M. Garbauskas and L. V. Interrante, *J. Am. Chem. Soc.*, 1986, **108**, 1908.
2 A. Kobayashi, H. Kim, Y. Sasaki, R. Kato, H. Kobayashi, S. Moriyama, Y. Nishio, K. Kajita and W. Sasaki, *Chem. Lett.*, 1987, 1819.
3 H. Tajima, M. Inokuchi, A. Kobayashi, T. Ohta, R. Kato, H. Kobayashi and H. Kuroda, *Chem. Lett.*, 1993, 1235.
4 L. Brossard, M. Ribault, L. Valade and P. Cassoux, *J. Phys. France*, 1989, **50**, 1521.
5 A. Kobayashi, H. Kobayashi, A. Miyamoto, R. Kato, R. A. Clark and A. E. Underhill, *Chem. Lett.*, 1991, 2163.
6 H. Kobayashi, K. Bun, T. Naito, R. Kato and A. Kobayashi, *Chem. Lett.*, 1992, 1909.
7 C. Faulmann, J.-P. Legros, P. Cassoux, J. Cornelissen, L. Brossard, M. Inokuchi, H. Tajima and M. Tokumoto, *J. Chem. Soc., Dalton Trans.*, 1994, 249.
8 R. Kato, T. Mori, A. Kobayashi, Y. Sasaki and H. Kobayashi, *Chem. Lett.*, 1984, 1.
9 R. Kato, H. Kobayashi, H. Kim, A. Kobayashi and Y. Sasaki, *Synth. Met.*, 1988, **27**, B359.
10 L. R. Groeneveld, G. J. Kramer, T. B. L. W. von Marinelli, H. B. Brom, J. G. Haasnoot and J. Reedijk, in *Organic and Inorganic Low-Dimensional Crystalline Materials*, ed. P. Delhaès and M. Drillon, Plenum Press, New York, 1987, pp. 349.
11 G. Steimecke, H.-J. Sieler, R. Kirmse and E. Hoyer, *Phosphorus Sulfur*, 1979, **7**, 49–55.
12 D. N. Hendrickson, Y. S. Sohn and H. B. Gray, *Inorg. Chem.*, 1971, **10**, 1560.
13 S. Alvarez, R. Vicente and R. Hoffmann, *J. Am. Chem. Soc.*, 1985, **107**, 6253.
14 G. J. Kramer and H. B. Brom, *Synth. Met.*, 1988, **27**, A133.
15 A. Kobayashi, H. Kim, Y. Sasaki, K. Murata, R. Kato and H. Kobayashi, *J. Chem. Soc., Faraday Trans.*, 1990, **86**, 361–369.